Archaeological and Anthropological Sciences (2026) 18:122
https://doi.org/10.1007/s12520-026-02487-5

RESEARCH

The ornamental stones of the Roman thermal baths of Teate Marrucinorum (Chieti, Italy): autoptic, geochemical and minero-petrographic multi-analytical characterisations

Arianna Casarin[1,2] · Fabrizio Antonelli[3] · Alessandro Cavallo[4] · Maria Rita Cicconi[5] · Maria Isabella Pierigè[6] · Emanuela Criber[6] · Francesco Radica[1,2] · Ilaria Capasso[1,2] · Maria Giovanna Masciotta[1,2] · Davide Potere[1] · Davide Rapone[1] · Dominique de Ligny[5] · Rosanna Tuteri[6] · Giuseppe Brando[1,2] · Gianluca Iezzi[1,2,7]

Received: 29 October 2025 / Accepted: 15 April 2026

Abstract
Ancient Romans exploited aesthetic natural stones from many sites across their Empire in the Mediterranean, transporting them for thousands of kilometres, to decorate their buildings. Petrographically, these metamorphic, sedimentary and igneous rocks display considerable differences, ranging from simple white stones to vividly coloured lithotypes. The source Region of these coloured stones is typically reconstructed from autoptic (visual and comparative examination of macroscopic or hand-sample scale) determinations, also taking advantage of the personal expertise of some specialists in the sector. Here, the ornamental stones of the 2nd-century AD thermal baths of *Teate Marrucinorum* (Chieti, Abruzzo region, Italy) are examined using a range of complementary methods. According to their autoptic features or mesoscopic textures, the initial 56 samples were divided into three categories: polychrome stones, grey-striped and white crystalline marbles. These rocks were analysed *via* bulk autoptic, mineralogical and geochemical methods; representative thin sections were also used for transmission optical microscope (TOM) petrographic and micro-Raman determinations. The $\delta^{18}O$ and $\delta^{13}C$ isotopic signatures were also characterised for white and grey-striped marbles. The complementary and multi-analytical approach unveils that the grey-striped marble is *Greco Scritto* (from Asia Minor), the white marbles come from Carrara (*Marmor Lunense*) and Marmara Island (*Marmor Proconnesium*) sources, whilst the four polychrome stones correspond *to Pavonazzetto Antico (Marmor Phrygium*), *Cipollino Verde* (*Marmor Carystium*), *Portasanta* (*Marmor Chium*) and *Breccia di Settebasi* (*Marmor Scyreticum*). The coupling of qualitative observations with quantitative measurements further constrains the provenance and features of the aesthetic rocks employed in the ancient town by the Romans.

Keywords Roman baths · Polychrome stones · White marbles · Autoptic · XRPD and XRF analyses

Introduction

Rocks and sediments have been exploited for millennia to decorate artefacts and obtain building materials. During Roman times, large quantities of stones were quarried and transported to build and decorate the external and internal surfaces of baths, theatres, villas, streets and monuments in general, as well as for statuary, either from surrounding areas or from many and faraway sites (Pensabene 1993, 2002). The importance of these activities and prices concerning

✉ Arianna Casarin
arianna.casarin@unich.it

1 Dipartimento di Ingegneria e Geologia (INGEO), Università degli Studi "G. d'Annunzio" di Chieti-Pescara, Pescara, Italy

2 UdA-TechLab, Research Center, University "G. d'Annunzio" of Chieti-Pescara, Chieti, Italy

3 Iuav University of Venice, Venice, Italy

4 Dipartimento di Scienze dell'Ambiente e della Terra (DISAT), Università degli Studi Milano Bicocca, Milan, Italy

5 Department of Materials Science and Engineering, Institut für Glas und Keramik, Friedrich-Alexander-Universität Erlangen-Nürnberg, Erlangen, Germany

6 Soprintendenza archeologia belle arti e paesaggio per le province di Chieti e Pescara, Chieti, Italy

7 Istituto Nazionale di Geofisica e Vulcanologia, Sezione di Roma, Italy

Published online: 04 May 2026

ornamental stones is marked by the "*Edictum de Pretiis Rerum Venalium"* (Diocletian, 301 AD) (Gnoli 1988). The Romans distinguished *Marmora*, i.e. stones susceptible to being polished (mirror-like surface), from *lapides*, which could not be polished. All these raw materials include (i) sedimentary rocks (e.g., tenacious limestones, conglomerates, breccias, travertines and alabasters), (ii) metamorphic lithotypes (like meta-breccias, marbles) and (iii) igneous rocks, both extrusive (e.g., lavas) and intrusive (e.g., granitoids) (Lazzarini 2007; Taelman et al. 2023). Petrographically, marbles are metamorphic rocks subdivided into pure and impure marbles if the carbonate minerals are >95 or >50 plus<95 vol%, respectively (Fettes and Desmons 2007). In archaeology and cultural heritage studies, as well as in current commercial use, marbles are instead frequently defined following the Latin meaning and thus unrelated to mineralogical and petrographic criteria; consequently, *marmora* are lithotypes characterised by high aesthetic, cutting and polishing properties, often divided into white or *stricto sensu* (*s.s.) versus* coloured or *lato sensu* (*l.s.*) (European Commission - Extra-Expo project 2015). Here, Roman white and polychrome marbles, along with a third grey-striped marble category, sampled from the *thermae* of the ancient *Teate Marrucinorum*, the modern city of Chieti, (Abruzzo, Italy) (Figs. 1a, b), are investigated through a multi-analytical approach. This investigation also sheds new light on the archaeological importance of this thermal bath, commissioned by a renowned family, characterised by a complex and sophisticated hydraulic engineering, representing a landmark for the entire region.

The identification and provenance of the polychromatic samples were first established across mesoscopic textural and structural attributes by (i) analysing polished rock slabs through specific autoptic expertise or (ii) using comparative criteria with well-known and previously catalogued samples and/or classical treatises (Corsi 1845; Gnoli 1988; Borghini 1989). By contrast, the provenances of marble *s.s.* samples require additional petrographic and stable $\delta^{13}C‰$ and $\delta^{18}O‰$ isotopic determinations, in line with the updated protocol for white marble and grey varieties (Lazzarini 2007; Antonelli et al. 2009a; Yavuz et al. 2011; Antonelli and Lazzarini 2013, 2015). In parallel, all three marble categories were also distinguished according to their microscopic textures and structures determined *via* TOM (transmission optical microscope) observations on representative thin sections. These results and conclusions were complemented with quantitative mineralogical (XRPD and Raman) and geochemical (XRF-EDS) determinations to provide further characteristics of these rocks. This study enriches the characterisation portfolio of *Greco scritto*, white marbles and some polychrome lithologies present in the *Teate Marrucinorum* thermae and other archaeological sites (Agostini and Rossi 2012). In general, it provides an extended and complementary quantitative approach to analyse Roman ornamental polychrome stones and to constrain their geochemical, mineralogical and petrographic attributes. The attained outcomes also complement the historical and archaeological significance of *Teate Marrucinorum*, since the provenance of decorative marbles straightforwardly mirrors the economic, commercial and social importance of cities in the framework of the Roman Empire.

Historical and Archaeological Context The Roman *Teate Marrucinorum*, the former city of Chieti, developed on an Italic settlement (Fig. 1a) favoured by its strategic geographic context which dominated the Aterno-Pescara valley and the Tiburtina Valeria Roman road (Agostini 2018). The *Teate Marrucinorum* settlement thrived upon the hill of the periadriatic belt of Abruzzo, made of Plio-Pleistocene permeable sandstones, overlaying poorly permeable claystones (ISPRA 2012); this geological association favoured the emergence of some natural springs nodal for ancient urban sites. In fact, the archaeological remains of *Teate Marrucinorum* include many important monuments, such as the Roman theatre and the Civitella's amphitheatre, the sacred area of the temples and thermal baths complex with the cisterns; the latter site was accurately decorated with aesthetic stony panels, pilasters and mosaic (Agostini et al. 2002). These thermal baths were built between the 1 st and 2nd century AD on the eastern slope of the hill (42° 20 × 50.579" N, 14° 10 × 5.46" E, WGS84, Fig. 1b) and associated with an extensive and nine-vaulted cistern system fed by waters tapped from a close spring (Fig. 1c, d). Unfortunately, this part of the ancient city underwent landslides and erosion, leading to the collapse of the eastern part of the complex (Agostini 2018).

Nowadays, the thermal baths and cisterns are constituted of a few rooms accessible *via* a staircase from a transverse corridor (*vestibulum*) that led, through a colonnaded entrance, to a large room, paved with mosaic decoration (the probable *apodyterium*) and connected by an aisle with the *praefurnium* to produce heat (Fig. 1c, d). Three chambers used for hot baths, a *tepidarium* and two *calidaria*, are in the southern part, while the room for cold baths (*frigidarium)*, equipped with semicircular tubs, is near the *apodyterium*, which was partially ruined after the landslide between the 2nd and 4th century AD (Adinolfi et al. 2019). The large rooms were decorated with polychrome marble slabs and mosaics of great value, large carved columns and refined sculptures, demonstrating the importance of *Teate Marrucinorum*.

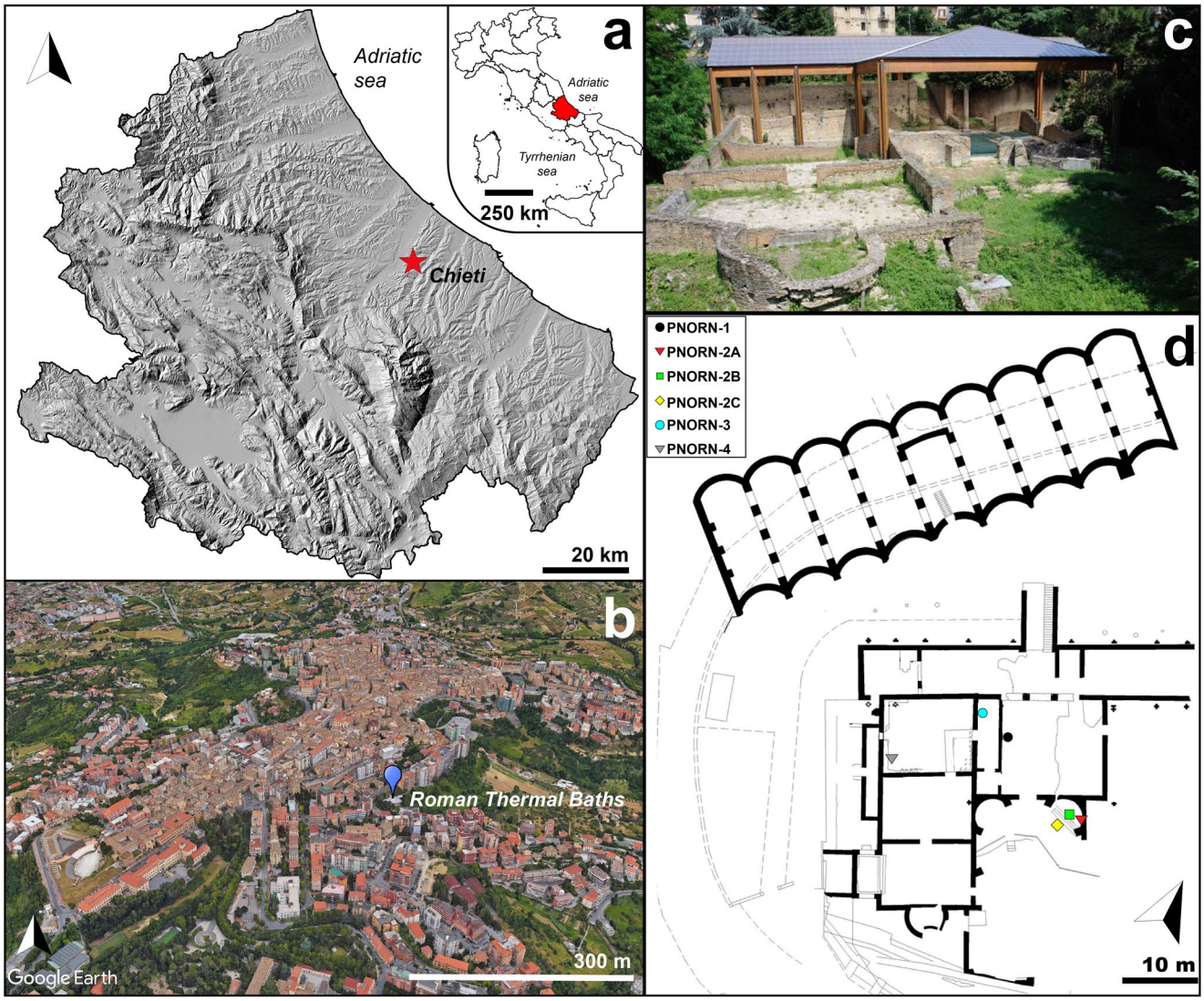

Fig. 1 (**a**) Geographical position of the city of Chieti and the Abruzzo region in Italy. DEM from Tinitaly, Tarquini et al. (2023); (**b**) 3D-view of the city of Chieti with the position of the Roman thermal baths (Map data from Google Earth Pro ©); (**c**) photo of the archaeological Roman thermal bath site and (**d**) its schematic plant. The original position inside the thermae of PNORN-X1 and PNORN-X2 groups is unknown; PNORN-2 C-1, PNORN-2 C-2 and PNORN-2 C-3 have the same location and are reported as PNORN-2 C, as well as PNORN-3, PNORN-3-A, PNORN-3-B, PNORN-3-C and PNORN-3-D that are reported as PNORN-3

Samples and Methods

We first collected 56 rock samples with a rectangular shape; only a fraction of them have a precise original location (Tab. S1), i.e. the specimens from the *tepidarium*, *apodyterium* and *frigidarium* that are respectively 1, 12 and 28, while those from unknown sites are 15 (Fig. 1d). These 56 rock fragments were sampled and divided into 3 main categories: 6 white marbles, 5 grey-striped marbles and 45 polychrome stones (Tab. S1). The specimens of the latter category were visually compared with the most similar and known ornamental catalogued samples according to an expert-based judgement; moreover, available images from several databases were considered from references or by comparing samples to images of polychrome stones previously identified. Due to their mesoscopic heterogeneity, each sample was first photographed and then divided into two halves: (i) one for further hand-specimen textural observations and Raman determinations and (ii) the other for producing homogeneous powders for XRPD and XRF-EDS analyses, as well as representative thin sections using as small as possible specimen, on the order of 5 × 5 × 1 cm (Figs. 2, S1). Nonetheless, the large size of several clasts in these rocks could results in variations of certain crystalline phases, especially the smallest ones, and consequently affect outcomes of bulk chemical and mineralogical

variations (on the order of < 0.5 wt%). Then, we powdered as large as possible specimen to attain the highest possible representativeness of XRF and XRPD results.

The microscopic textural (number, abundance, colour, size, shape and boundary of mineralogical phases) and structural (arrangement of phases in space) features were analysed using a polarised transmission optical microscope (TOM) Zeiss Axioskop 50 (Dept. INGEO, University "G. d'Annunzio"). The microscope is equipped with a Qimaging MicroPublisher 3.3 RTV digital camera linked to a computer with image analysis software Image-Pro Plus v.6.0 (Media Cybernetic Inc.) (Potere et al. 2023; Radica et al. 2024). Although the microscopic features are usually investigated only for white marble samples (marble *s.s.*), they are considered here for every stone. The dimension of the largest carbonate crystal (calcite/dolomite) (i.e. the Maximum Grain Size, MGS) was measured for every stone, thus expanding the number of quantitative parameters and enabling the existing databases.

Bulk rock geochemistry of powdered samples, i.e. major and minor oxides, was quantified with a PANalytical Epsilon 3-XL X-ray fluorescence energy-dispersive spectrometer (XRF-EDS) (University of Milano-Bicocca). The X-ray source is a Rh anode operating at variable kV (4 to 50) and µA (1 to 3000) conditions. Loss on ignition (LOI) was determined by heating the samples at 1050 °C for 5 h. The collected data were preliminarily analysed with the Malvern Panalytical Epsilon 3 software platform, using the Omnian-standardless model, which allows qualitative and quantitative chemical analysis of unknown materials without the construction of calibration curves. The quantitative analysis was then repeated in 6 different instrumental conditions, using the Panalytical WROXI® – synthetic, high-quality Certified Reference Materials for calibration.

Stable isotope ratios of oxygen and carbon were assessed using a Gasbench II preparation system coupled to a ThermoFinnigan Five Plus mass spectrometer operating in continuous flow mode, following the protocol described by McCrea (1950). The analysed powders were reacted with pure phosphoric acid at 70° C. Isotopic ratios are reported as $\delta^{13}C‰$ and $\delta^{18}O‰$ values relative to the Vienna-Pee Dee Belemnite (V-PDB) standard. These ratios were compared with the published isotopic databases for white marbles (Antonelli and Lazzarini 2015) and *Greco scritto* varieties (Cap de Garde, Algeria, Antonelli et al. 2009a; Hasançavuşlar, Turkey, Yavuz et al. 2011). Archaeological samples of *Greco Scritto* of Murecine (Perna et al. 2023) and Volubilis site (Antonelli et al. 2009b) are even plotted for comparison.

X-ray powder diffraction (XRPD) was carried out with an X'Pert PRO PANalytical diffractometer in Bragg-Brentano geometry (University of Milano-Bicocca). Each pattern was recorded in the 3°−71° angular range of 2θ, with a step size of 0.02° and a counting time of 2 s/step; the Cu Kα1 = 1.5406 Å incident radiation was produced with 40 kV and 40 mA. Data elaboration was performed with X'Pert Highscore v.2.1 software (Malvern Panalytical, Malvern, UK), using the ICDD PDF2-2004 database, following the typical search-match procedure reported in several other studies (Iezzi et al. 2003; Della Ventura et al. 2005). A semi-quantitative evaluation of the abundance of crystalline phases (wt%) was assessed using the Reference Intensity Ratio (RIR) method (Hubbard and Snyder 1988; Chipera and Bish 2013), through which the intensity scaling factor of each mineralogical phase (I) was compared with a "virtual" corundum crystalline phase ($I_{cor.}$) not necessarily present in the XRPD patterns. Then, the semi-quantitative content (wt%) of each crystalline phase is pursued by the ratio "I/I_{cor}" (Galderisi et al. 2022).

The XRPD results were complemented by unpolarised Raman spectroscopy measurements carried out on a few μm^2 portions of the specimens, allowing the textural identification of the most prominent carbonate and silicate minerals. Spectra were collected in the frequency range of 30–1550 cm^{-1} using a coherent sapphire single-frequency 488 nm laser as excitation source, and an iHR 320 Horiba spectrometer coupled with a Sincerity UV–Vis CCD camera (Institut für Glas und Keramik, Erlangen). The black crosses shown in the photos in Fig. 2 represent the Raman spots. For each sample, between 8 and 12 different spots were investigated with an OptoSigma PAL-50-L NA 0.42 objective. Spectra were background-subtracted with a linear function and normalised to the total area. $CaCO_3$ (Sigma Aldrich) was measured as well under the same conditions and used as a reference.

Results

Autoptic Determinations The polychrome stones present different fabrics (textural and structural characteristics) (Fig. 2). PNORN-1 shows a brecciated structure, with large purple veins that run across the white marble clasts; these clasts have a saccharoidal texture. PNORN-2 A presents cm-sized parallel to slightly curved bands with alternating greenish to whitish tones; the texture is saccharoidal (Fig. 2). PNORN-X1 group is visually variable; it shows a brecciated aspect, composed of mm- to cm-sized white to dark red clasts closely in contact, in a pinkish to red scarce matrix. These clasts are angular and some of them can reach pluri-cm to decimetre size (Fig. 2). PNORN-2 C-1 and PNORN-2 C-2 samples show similar characteristics, with many large, closely spaced and deformed, angular white clasts (from a few to many cm) in a dark red to black matrix (Fig. 2). PNORN-2 C-3 samples also show

Fig. 2 Mesoscopic surfaces of the analysed specimens: (i) polychrome samples: PNORN-1, PNORN-2 A, PNORN-2 C-1, PNORN-2 C-2, PNORN-2 C-3, PNORN-4, PNORN-X1; (ii) grey-striped marbles: PNORN-3, PNORN-3-A, PNORN-3-B, PNORN-3-C, PNORN-3-D and (iii) white marbles: PNORN-2B, PNORN-X2, PNORN-X2-A, PNORN-X2-B, PNORN-X2-C, PNORN-X2-D. The half part with black crosses was used to collect Raman data and to obtain thin sections; some flakes on the order of 25 cm^3 detached from the remaining half were exploited to produce powder for XRPD and XRF-EDS analyses

similar characteristics, plus yellowish to dark red clasts with angular to sub-angular contours (Fig. 2). In all the PNORN-2 C samples clasts are often iso-aligned and define a clear foliation. Compared to all the other rock samples, PNORN-4 has much darker hues due to the amount of the matrix; the white to dark red angular clasts have limited size respect to the other polychrome samples and seems more deformed (Fig. 2). Autoptic analysis indicates that rocks of the thermal baths of *Teate Marrucinorum* correspond to 4 well known lithotypes: *Pavonazzetto antico* (*Marmor Phrygium*, PNORN-1), *Cipollino Verde (Marmor Carystium*, PNORN-2 A), *Portasanta (Marmor Chium*, PNORN-X1) and *Breccia di Settebasi* (*Marmor Scyreticum*, PNORN-2 C-1, PNORN-2 C-2, PNORN-2 C-3 and PNORN-4) (Tab. S2 and Fig. 2). These outcomes corroborate with previous determinations reported in Agostini et al. (2002). The grey striped marbles (PNORN-3 series, Tab. S2) exhibit a white background with numerous dark to light grey, thin, deformed (micro-crenulated) layers, typical of the *Greco scritto* marble varieties (Fig. 2). Instead, the third category of white marbles cannot be determined only by their mesoscopic appearance. PNORN-2B, PNORN-X2 and PNORN-X2-C exhibit a white tending towards pale grey or bluish tones, frequently with carbonaceous/graphitic planar foliation or crossed by linear grey veins, whereas PNORN-X2-A, PNORN-X2-B and PNORN-X2-D samples show a homogenous fine grain-size matrix with warmer white tone, often with ivory or milky hues; the former three samples have calcite crystals larger than the latter three ones (Fig. 2).

TOM TOM observations reflect the first qualitative autoptic observations (Tab. S2). Calcite crystals are by far the most abundant mineral in all samples, according to XRPD outcomes (see below and Figs. 3). PNORN-1 (*Pavonazzetto antico*) is a marble that shows a heteroblastic texture with embayed crystals up to an MGS of 2.7 mm, plus polysynthetic twinning sometimes showing intracrystalline deformation, mosaic microstructure and recrystallised calcite in veins; tiny and sparsely distributed opaque to black/brown/reddish unidentifiable (by TOM) phases also occur (Fig. S2). Calcite crystals in *Cipollino verde* marble (PNORN-2 A) vary from hetero- to homeoblastic, with an MGS of 2.1 mm, a lineated microstructure and embayed crystal boundaries. Along the foliation planes, grey to green phyllosilicates (white mica and chlorite) are located, visible at both the mesoscopic and microscopic scales (Fig. 2, S2). Additionally, some quartz crystals and opaque minerals are present. All the other polychrome stones are brecciated, with carbonate clasts made of micritic to cryptocrystalline calcite (Tab. S2 and Fig. S2). The PNORN-X1 *Portasanta* is a brecciated limestone with a clastic texture; the angular clasts are referrable to a mudstone made of micritic calcite, scarcely recrystalized; these breccia elements are closely in contact; they can be separated by a scarce matrix (having similar textural features of the clasts) or by dark stylolithic features. Few clasts show the presence of ooids and peloids. Although the PNORN-X1 (*Portasanta*) is not a metamorphic rock, we measured though the dimensions of the largest calcite crystal (1.6 mm) present in the thin section (referred as a sedimentary MGS, see below), corresponding to a slightly recrystallized portion of the micritic matrix. The meta-breccia labelled *Breccia di Settebasi*, corresponding to the PNORN-2 C-1, PNORN-2 C-2, PNORN-2 C-3 and PNORN-4 samples, display brecciated, clastic structure; the angular, elongated and iso-aligned breccia elements are marble clasts made of fine calcitic crystals, i.e., ~ 0.06 to 0.2 mm in size (Fig. S2 and Tab. S2) showing an homeoblastic texture. These marble clasts show some zones in which there are a few larger calcite crystals; according to Lazzarini (2007), the MGS for these samples can consider the recrystallisation in these portions of the clasts; following this approach, the MGS are 0.8, 0.7, 1.7 and 2.4 mm for PNORN-2 C-1, PNORN-2 C-2, PNORN-2 C-3 and PNORN-4, respectively (Tab. S2 and Fig. S2). In addition, larger calcite porphyroclasts are well visible, as they are separated by dark layers hosting tiny, reddish to black crystals.

Greco scritto sample PNORN-3 has a heteroblastic texture with embayed to sutured calcite crystals, polysynthetic

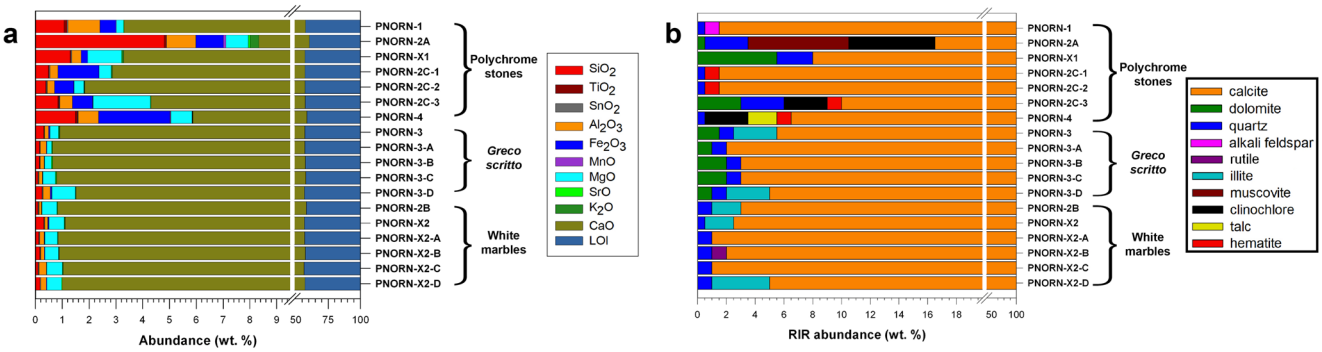

Fig. 3 (**a**) Oxide abundance determined by XRF-EDS plus LOI (see Tab. S3). (**b**) Abundance of crystalline phases determined by RIR (wt%) in the four polychrome stones, *Greco scritto* and white marble samples (see Tab. S4)

twinning, a mosaic microstructure and a MGS of 2.7 mm (Tab. S2 and Fig. S2); this sample also shows levels of undeterminable coloured/opaque phases, hosting possibly also carbonaceous material(s) (Fig. 2). PNORN-2B, PNORN-X2 and PNORN-X2-C white marble samples have heteroblastic texture. PNORN-2B has a mortar microstructure with embayed to sutured calcite boundaries and a MGS of 3.7 mm (Tab. S2 and Fig. S2). PNORN-X2 and PNORN-X2-C have similar characteristics (mortar microstructure, embayed to sutured crystal boundaries); MGS is 2.6 mm and 2.9 mm, respectively (Tab. S2 and Fig. S2). PNORN-X2-A has a texture mainly homeoblastic, somewhere passing to heteroblastic, mosaic microstructure and curved to straight crystal boundaries, with calcite crystals having a maximum size of 0.8 mm (Tab. S2 and Fig. S2). PNORN-X2-B and PNORN-X2-D are both homeoblastic, characterised by a mosaic microstructure with both straight and curved crystal boundaries (Tab. S2 and Fig. S2). PNORN-X2-B tends to show a polygonal texture, with triple joints and its MGS is 0.7 mm, whereas in PNORN-X2-D triple joints are rare, with the maximum size of calcite of 0.6 mm (Tab. S2 and Fig. S2).

XRF-EDS Bulk oxide compositions of all the samples are plotted in Fig. 3a and compiled in Tab. S3. The sum of CaO and LOI (*Loss On Ignition*) is invariably higher than 90 wt% (CaO: 52.1 to 57.4 wt%), while the other oxides sum up between 0.6 and 8.3 wt%. CaO + LOI is the lowest and the highest for the *Cipollino verde* PNORN-2 A and the *Greco scritto* PNORN-3-B, respectively (Fig. 3a). Polychrome stones show higher values of $SiO_2 + Al_2O_3 + Fe_2O_3 + MgO$ (7.7 wt% for *Cipollino*, 3.2 wt% for *Pavonazzetto*, PNORN-1; PNORN-2 A; 3.1 wt% for *Portasanta*, PNORN-X1; from 1.8 wt% to 5.8 wt% for *Breccia di Settebasi*, PNORN-2 C-1, PNORN-2 C-2, PNORN-2 C-3 and PNORN-4) compared to *Greco scritto* (0.6–1.5 wt%) and white marble varieties (0.8–1.8 wt%) (Fig. 3a). Bulk compositions of white marbles and *Greco scritto* marbles are similar to each other, with PNORN-3-D having the relatively highest MgO and lowest CaO contents (Fig. 3a). The highest amount of SiO_2 is reached by *Cipollino verde* (PNORN-2 A, SiO_2: 4.8 wt%) and in general, is higher for polychrome samples (from 0.4 wt% to 1.5 wt%) and lower for *Greco scritto* and white marbles (Fig. 3a). Al_2O_3 is relatively high in *Pavonazzetto* and *Cipollino* (PNORN-1 and PNORN-2 A); the highest Fe_2O_3 and MgO amounts are in *Breccia di Settebasi* PNORN-4 and PNORN-2 C-3, respectively (Fig. 3a and Tab. S3). SnO_2 and MnO are invariably below the detection limit (LOD ~ 0.05 wt%), except for *Cipollino verde* (MnO: 0.10 wt%); TiO_2 is appreciable only for *Cipollino verde*, *Pavonazzetto* and PNORN-4 *Breccia di Settebasi*. Again, K_2O and SrO are both detectable in *Cipollino*, while K_2O and SrO are individually present in *Portasanta* and PNORN-3-B *Greco scritto*, respectively (Tab. S3).

Stable Isotopes of Oxygen and Carbon The stable C and O isotope ratios of white marble samples are reported in Tab. S3 and plotted in Fig. 4, in two plots corresponding to fine-grained (MGS ≤ 2.00 mm) and medium- to coarse-grained (MGS > 2.00 mm) white marbles. Isotopic $\delta^{18}O$ and $\delta^{13}C$ ratios of medium-grained samples are respectively − 1.54‰ and 2.18‰ for PNORN-2B, −2.03‰ and 2.75‰ for PNORN-X2, −2.31‰ and 3.50‰ for PNORN-X2-C (Fig. 4). Marble varieties having MGS ≤ 2.00 mm have stable isotope values of −1.83‰ and 2.25‰ (PNORN-X2-A), −2.19‰ and 2.34‰ (PNORN-X2-B), −1.95‰ and 2.24‰ (PNORN-X2-D) for $\delta^{18}O$ and $\delta^{13}C$, respectively (Fig. 4). *Greco scritto* specimens (PNORN-3 series) have $\delta^{18}O$ ranging from −3.03‰ to −2.52‰ (PNORN-3-C and PNORN-3-D, respectively), while minimum and maximum values for $\delta^{13}C$ are 2.26‰ (PNORN-3-D) and 4.22‰ (PNORN-3-B) (Tab. S3 and Fig. 4).

XRPD The XRPD patterns of the analysed stones are stacked in Figs. S3a, b, along with recognised minerals; the single XRPD patterns are reported in Fig. S5 to Fig. S22. The background is invariably flat and the Bragg reflections are extremely sharp and intense, indicating that all phases are highly crystalline and amorphous material is absent (Fig. S5 to Fig. S22). Calcite invariably shows the most intense Bragg peaks (Figs. S3a, b). The abundance of phases in wt% per sample is tabulated in Tab. S4; the RIR quantification indicates that calcite ranges from 83.5 wt% (PNORN-2 A) to 99.0 wt% (PNORN-X2-A and PNORN-X2-C) (Fig. 3b), whereas dolomite is relatively significant only for PNORN-X1 (*Portasanta*) and *Breccia di Settebasi* PNORN-2 C-3, the two samples with the highest amounts of MgO (Figs. 3a, b). However, in other *Breccia di Settebasi* samples, dolomite is absent (Tab. S4). Lazzarini (2007) attributes the presence of dolomite in *Portasanta* and *Breccia di Settebasi* marbles to its occurrence within only a few of their clasts. In *Greco scritto*, dolomite varies from 1 to 2 wt%, while it is lacking in all white marble varieties (Tab. S4). The amount of quartz is low but present in all samples; it attains 0.5 wt% in *Pavonazzetto* PNORN-1 and in *Breccia di Settebasi* samples, except for PNORN-2 C-3, in which it arrives at 3 wt% (Tab. S4). In *Portasanta* and *Cipollino verde*, the quartz content is 2.5 wt% and 3.0 wt%, respectively, while it is constant at 1 wt% for white (less in PNORN-X2, qtz: 0.5 wt%) and *Greco scritto* marbles (Tab. S4). Alkali-feldspars are also low but detectable for PNORN-1 (Tab. S4). *Cipollino verde* is also rich in muscovite and clinochlore in line with the highest SiO_2; similarly, PNORN-2 C-3 and PNORN-4 samples have 3.0 wt% clinochlore, while PNORN-4 hosts talc

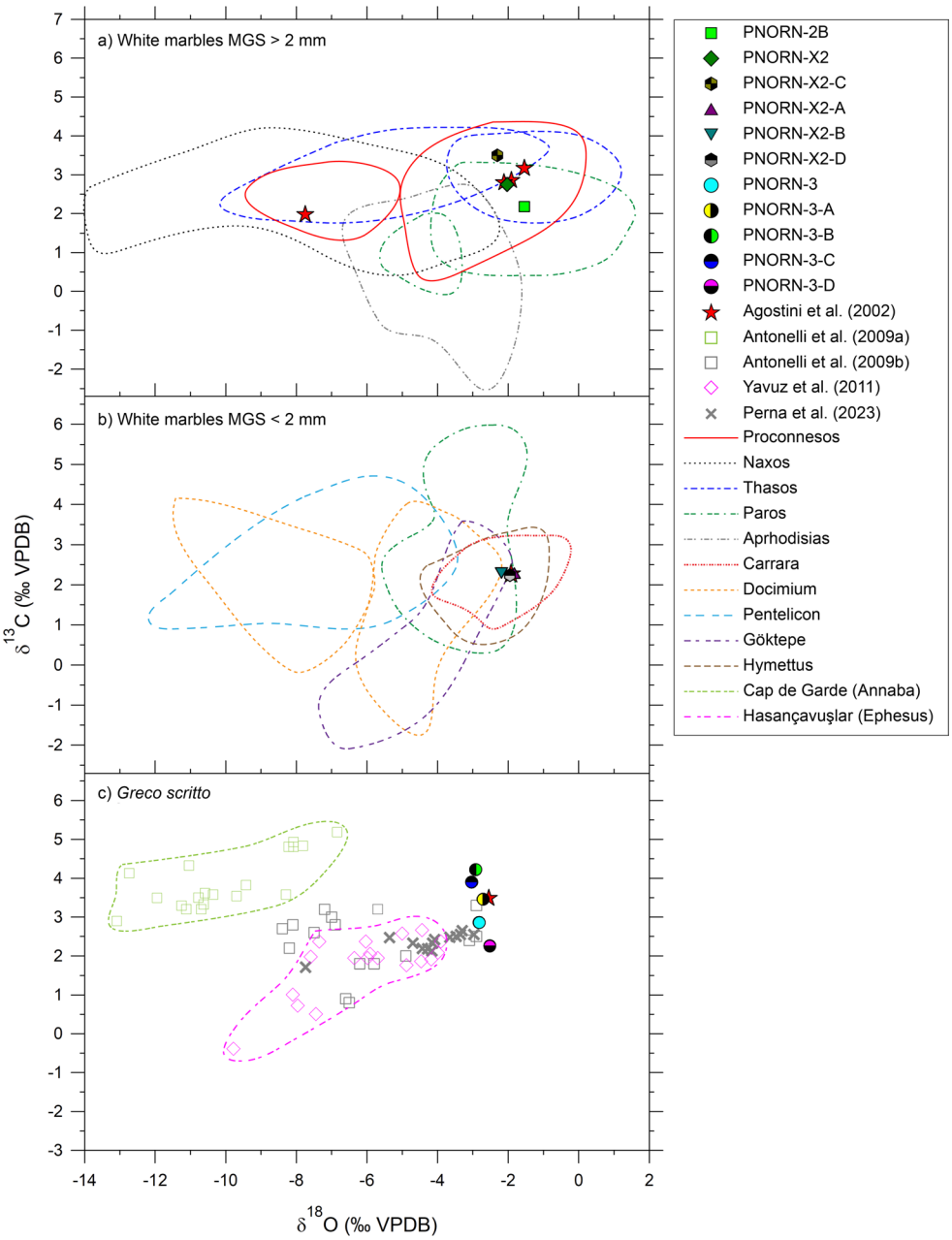

Fig. 4 Isotopic signature of analysed marbles (see Tab. S3). White marbles having (**a**) MGS > 2 mm (samples PNORN-2B, PNORN-X2, PNORN-X2-C) and (**b**) MGS ≤ 2 mm (samples PNORN-X2-A, PNORN-X2-B, PNORN-X2-D) (Antonelli and Lazzarini 2015); (**c**) *Greco scritto* samples (PNORN-3, PNORN-3-A, PNORN-3-B, PNORN-3-C, PNORN-3-D). The reference databases for quarry raw materials from Cape de Garde (Annaba, Algeria) and Hasançavuşlar (Ephesus, Turkey) are Antonelli et al. 2009a); Yavuz et al. (2011), respectively. Whereas those from Murecine (Perna et al. 2023) and Volubilis sites (Antonelli et al. 2009b) are archaeological samples. Isotopic determinations from Agostini et al. (2002) are shown as red stars

(Tab. S3 and Fig. 3a). Illite is 3.0 wt% in *Greco scritto* PNORN-3 and PNORN-3-D; it is also detectable in medium-grained marbles PNRON-2B and PNORN-X2; it attains 4.0 wt% in PNORN-X2-D fine-grained white marble (Tab. S4). Finally, hematite is detected in the four *Breccia di Settebasi*, while rutile is present only in PNORN-X2-B.

Raman Spectroscopy The micro-Raman data (Tab. S4 and Fig. S4) complement the XRPD results and enable the correlation of textural features with crystal–chemical attributes in the polychrome rocks and the *Greco scritto* sample PNORN-3. The individual Raman spectra are displayed in Fig. S23 to Fig. S29. As expected, calcite displays the most intense Raman vibration centred at ~1090 cm^{-1} (black spectra in Fig. S4), but some other faint vibration modes are also present (red spectra in Fig. S4). In agreement with XRPD results, the *Pavonazzetto* specimen PNORN-1 exhibits the presence of alkali-feldspars, whereas the spectra of *Cipollino* and *Portasanta* (PNORN-2 A and PNORN-X1, respectively) reveal the presence of quartz (Fig. S4). Unexpectedly, aragonite was detectable exclusively by Raman in PNORN-4 (*Breccia di Settebasi* specimen), which is also the only sample in which Fe oxides/hydroxides (attributable to hematite) could be identified (Fig. S4). Consistent with the XRPD data, in *Greco scritto* PNORN-3, dolomite was detected. Sheet-silicates are not detected by Raman

spectroscopy, possibly due to their fine grain sizes and/or high localisation within domains.

Discussion

White and Greco Scritto Marbles The isotopic comparisons of white and grey-striped marbles with those present in reference databases are reported in Fig. 4, along with mineralogical (Fig. 3b, Fig. S3, S4) and especially petrographic (Tab. S2 and Fig. S2) parameters. Crucially, petrographic characteristics of the analysed marbles resolve isotopic overlaps among marble sources located in the same field of the isotopic plots (Tab. S2). Specifically, specimens PNORN-2B, PNORN-X2, and PNORN-X2-C were compared against isotopic values for medium- to coarse-grained marbles (MGS > 2 mm, Fig. 4). Their isotopic signatures plot within three distinct fields: Proconnesian, Parian, and Thasian. These three samples from *Teate Marrucinorum* exhibit a heteroblastic, mortar microstructure with embayed-to-sutured crystal boundaries (Tab. S2), that are diagnostic features of Proconnesian marble. Provenance from Paros or Thasos is excluded by the absence of curved boundaries and mosaic microstructures (Fig. S2). Conversely, the fine-grained sample (MGS ≤ 2 mm, Fig. 4) PNORN-X2-A falls within both the Carrara and Hymettan fields. However, the presence of straight and curved calcite boundaries, combined with the lack of lineated microstructure, excludes a Greek origin in favour of a Lunense (Carrara) provenance (Tab. S2 and Fig. S2). Similar logic applies to PNORN-X2-B and PNORN-X2-D. While their isotopic values are consistent with several sources (Carrara, Hymettus, Paros, Docimium, and Göktepe), their constant homeoblastic texture and triple junctions point toward an Italian origin. (Tab. S2 and Fig. S2). These dual provenances (Carrara for *Marmor Lunense* and Marmara Island for *Marmor Proconnesium*) corroborate the previous findings of Agostini et al. (2002).

The provenance of the *Greco scritto* was instead undetermined in Agostini et al. (2002); our new isotopic results strongly suggest an Asia Minor provenance (Fig. 4), considering the provenance areas resulted from quarried raw materials reported in Antonelli et al. (2009a) for Cape de Garde provenance (Annaba, Algeria) and Yavuz et al. (2011) for Hasançavuşlar (Ephesus, Turkey). Additionally, to have a comparison with other archaeological specimens, the isotopic values of Murecine samples of Perna et al. (2023) and that from Volubilis site (Antonelli et al. 2009b) are also shown. In Fig. 4 our *Greco scritto* samples (PNORN-3, PNORN-3-A, PNORN-3-B, PNORN-3-C, PNORN-3-D) plus one from Agostini et al. (2002) plot close to the isotopic field recorded for marble from the Microasiatic quarry of Hasançavuşlar (Yavuz et al. 2011); furthermore, also our new TOM determinations match with an Ephesian origin for the *Greco scritto* samples of *Teate Marrucinorum*. Importantly, these data coupled with those reported in Antonelli et al. (2009b) and those recently published by Perna et al. (2023) suggest a possible enlargement of the Hasançavuşlar *Greco scritto* field towards higher $\delta^{18}O$ and $\delta^{13}C$ ratios (Fig. 4).

Polychrome Stones The polychrome stones are typically recognised only *via* autoptic determinations. Here, we compare and complement this aspect (Fig. 2) with geochemical (Fig. 3a and Tab. S3), mineralogical (Fig. 3b, Figs. S3, S4 and Tab. S4) and petrographic (Fig. S2 and Tab. S2) quantitative parameters. The *Pavonazzetto* polychrome PNORN-1 specimen is a pure crystalline marble *s.s.* (Tab. S2 and Fig. S2) due to its calcite > 95 wt% with only minor alkali-feldspars and quartz (Figs. 3b, S3, S4 and Tab. S4); its heteroblastic mosaic texture is made of calcite grains with embayed contours and a MGS of 2.7 mm (Tab. S2, Fig. S2). These features are corroborated by high CaO and LOI, coupled with SiO_2 and Al_2O_3 contents close to 1 wt% (Fig. 3a, Tab. S3). The opposite situation is presented by the impure (calcite < 95%) *Cipollino verde* PNORN-2 A marble, the poorest in calcite (~84 wt%) and the richest for the other remaining four minerals, i.e. dolomite, quartz, muscovite and clinochlore (Figs. 3b, S3, S4 and Tab. S4); coherently, the amount of $SiO_2+Al_2O_3+Fe_2O_3+MgO$ is the highest (Fig. 3a, Tab. S3). This stone has calcite grains invariably with embayed boundaries, displaying a (prevalently) heteroblastic mosaic texture; it is the unique rock with an anisotropic fabric and attains an MGS close to 2.1 mm (Tab. S2, Fig. S2). The *Portasanta* PNORN-X1 has the largest content of dolomite (5.5 wt%) and a low, but significant amount of quartz (Figs. 3b, S3, S4 and Tab. S4); this paragenesis corroborates the relatively high contents of both SiO_2 and MgO > 1 wt% (Fig. 2, Tab. S3). Petrographically, the PNORN-X1 is a sedimentary calcitic tectonic breccia without or with a very poor amount of matrix. It is characterised by a brecciated texture made of clasts of very fine micritic and more rarely sparitic limestone; the sedimentary MGS up to 1.6 mm (Tab. S2, Fig. S2). The four *Breccia di Settebasi* (PNORN-2 C-1, PNORN-2 C-2, PNORN-2 C-3 and PNORN-4) samples are the same meta-breccia (Tab. S5), although they appear different in hand-specimen at least for an unexpert eye (Fig. 2); in fact, they represent the different facies of the same metamorphic lithotype derived from a detrital sedimentary rock. They have the same brecciated and textural attributes as the marbles' clasts; however, their MGS measurements range from 0.7 to 2.4 mm (Tab. S2, Fig. S2). These similarities are further agreed by their mineral contents, since quartz and hematite occur in all these stones; in addition, PNORN-2 C-3 and PNORN-4 host

also clinochlore, plus only dolomite in PNORN-2 C-3 and talc for PNORN-4 (Figs. 3b, S3 and Tab. S4). These slight mineralogical differences are also reflected by SiO_2, Al_2O_3, Fe_2O_3 and MgO variations. These low but detectable geochemical, mineralogical and MGS differences are related to heterogeneities of the same original lithotype.

Comparisons of Mineralogical, Geochemical and MGS Data from the Literature The differentiation of several ornamental Roman stones could be challenging to an inexperienced researcher. Thereby, to complement and further corroborate autoptic determinations, we compare the mineralogical, geochemical and MGS salient attributes of the lithotypes from the Roman thermal baths of *Teate Marrucinorum* (Chieti, Italy) (Figs. 5, 6 and 7). This approach could help integrate and enlarge the few existing databases to characterise these stones further. The mineralogy of white marbles and *Greco scritto* are mainly made of calcite (>94 wt%) plus minor amounts of dolomite (only *Greco scritto*, ≤ 2 wt%) and quartz±illite±rutile, invariably≤5 wt% (Tab. S4); conversely, *Pavonazzetto*, *Cipollino verde* and *Breccia di Settebasi* polychrome stones host alkali-feldspar (*Pavonazzetto*), muscovite+clinochlore (≤13 wt%), hematite±talc clinochlore (≤6 wt%), respectively, in addition to calcite, quartz and eventually dolomite (Tab. S4).

In Fig. 5, two coupled triangular diagrams and six binary plots of oxide ratios (SiO_2/Fe_2O_3, SiO_2/Al_2O_3, SiO_2/MgO, Al_2O_3/Fe_2O_3 and Al_2O_3/MgO) are displayed, allowing a straightforward visualisation and discrimination of compositional clusters from isolated ones (Fig. 5). The polychrome *Pavonazzetto* sample (PNORN-1, black circle in Fig. 5) is invariably well separated in any of these eight plots, showing the highest value of Al_2O_3 between the polychrome samples. The *Cipollino verde* (PNORN-2 A, red triangle in Fig. 5) is also perfectly separated from any other stones, except in the triangular SiO_2 vs. Fe_2O_3 vs. Al_2O_3 and in the SiO_2/Fe_2O_3 vs. SiO_2/Al_2O_3 plots, where it overlaps with the *Portasanta* (PNORN-X1, dark red square in Fig. 5). The *Portasanta* (PNORN-X1, dark red square in Fig. 5) sample is the poorest in Fe_2O_3 content between polychrome ornamental stones analysed here; it is poorly discriminable from other Roman stones, except in the plots SiO_2/MgO vs. SiO_2/Al_2O_3 and Al_2O_3/MgO vs. SiO_2/Al_2O_3 (Fig. 5). The *Breccia di Settebasi* stones, i.e. PNORN-2 C-1, PNORN-2 C-2, PNORN-2 C-3 and PNORN-4 (yellow diamond, blue

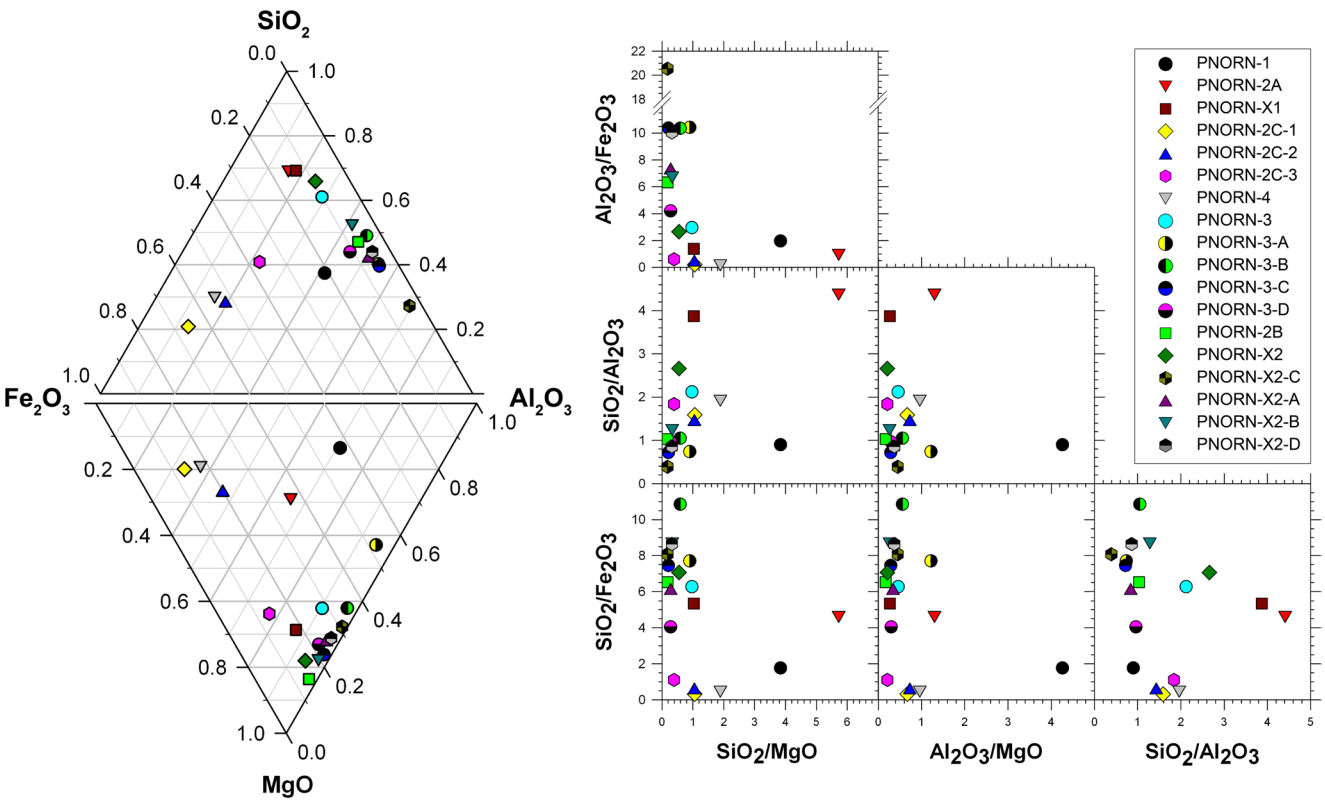

Fig. 5 Major oxides triangular (left) and binary ratios (right) plots for the ornamental stones of the thermal baths of *Teate Marrucinorum*. See the text for a more detailed discussion

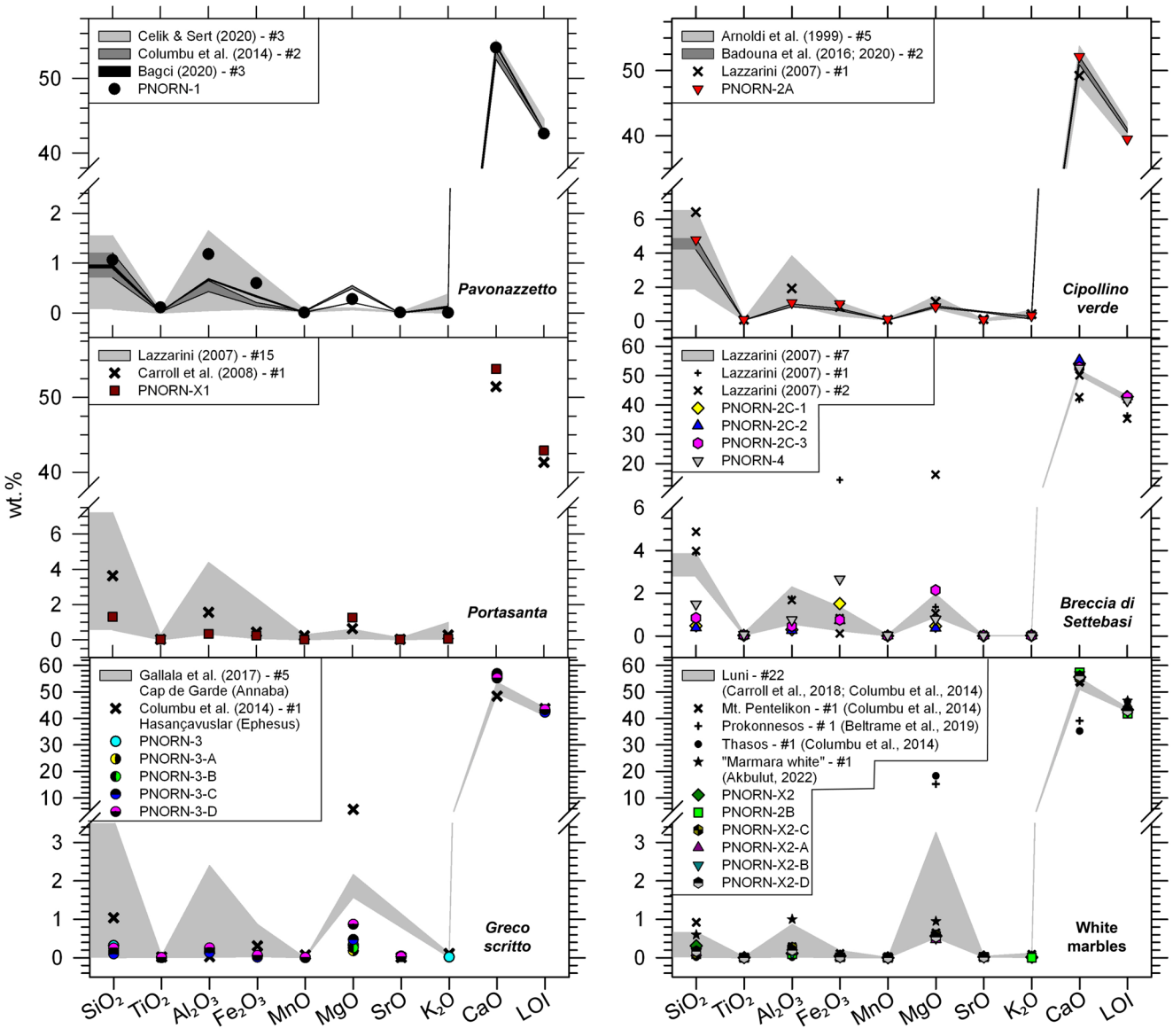

Fig. 6 Comparison of bulk chemical compositions of the lithotypes investigated here with those available in the literature (Akbulut 2022; Arnoldi et al. 1999; Badouna et al. 2016, 2020; Bağci 2020; Beltrame et al. 2019; Carroll et al. 2008; Çelik and Sert 2020; Columbu et al. 2014; Gallala et al. 2017; Lazzarini 2007)

triangle, pink hexagon and grey triangle, respectively, in Fig. 5) are all clustered and isolated from other samples in the SiO_2 vs. Fe_2O_3 vs. Al_2O_3 triangular plot, plus the SiO_2/MgO vs. the SiO_2/Fe_2O_3, Al_2O_3/MgO vs. SiO_2/Fe_2O_3 and SiO_2/Al_2O_3 vs. SiO_2/Fe_2O_3 binary plots (Fig. 5). The other white varieties and *Greco scritto* stones have a primary geochemical distinction from the polychrome stones since they have invariably (very) lower amounts of Fe_2O_3 (both triangular plots of Fig. 5, Tab. S3 of the Online Resource 1); by contrast, they are wholly or poorly discriminable among themselves in both triangular and binary diagrams (Fig. 5).

Below, these previous data are considered together with geochemical plus MGS (Figs. 6 and 7); such comparisons are limited in the literature for polychrome stones and therefore we also considered decorative marbles from modern excavations. In Fig. 8 and Tab. S5, the provenance sites, ancient name, petrographic type and possible quarries of the ornamental stones of the thermal baths from *Teate Marrucinorum* (Chieti, Italy) are resumed. The whole chemistry compositions of white marble are similar between the different varieties considered for the comparison, with only minor discrepancies for the MgO and CaO (Fig. 5); the same situation is also valid for the various *Greco scritto* rocks (Fig. 6). Again, the major oxides of polychrome *Pavonazzetto*, *Cipollino verde* and *Portasanta* stones analysed here overlap with those from literature; in contrast, the *Breccia*

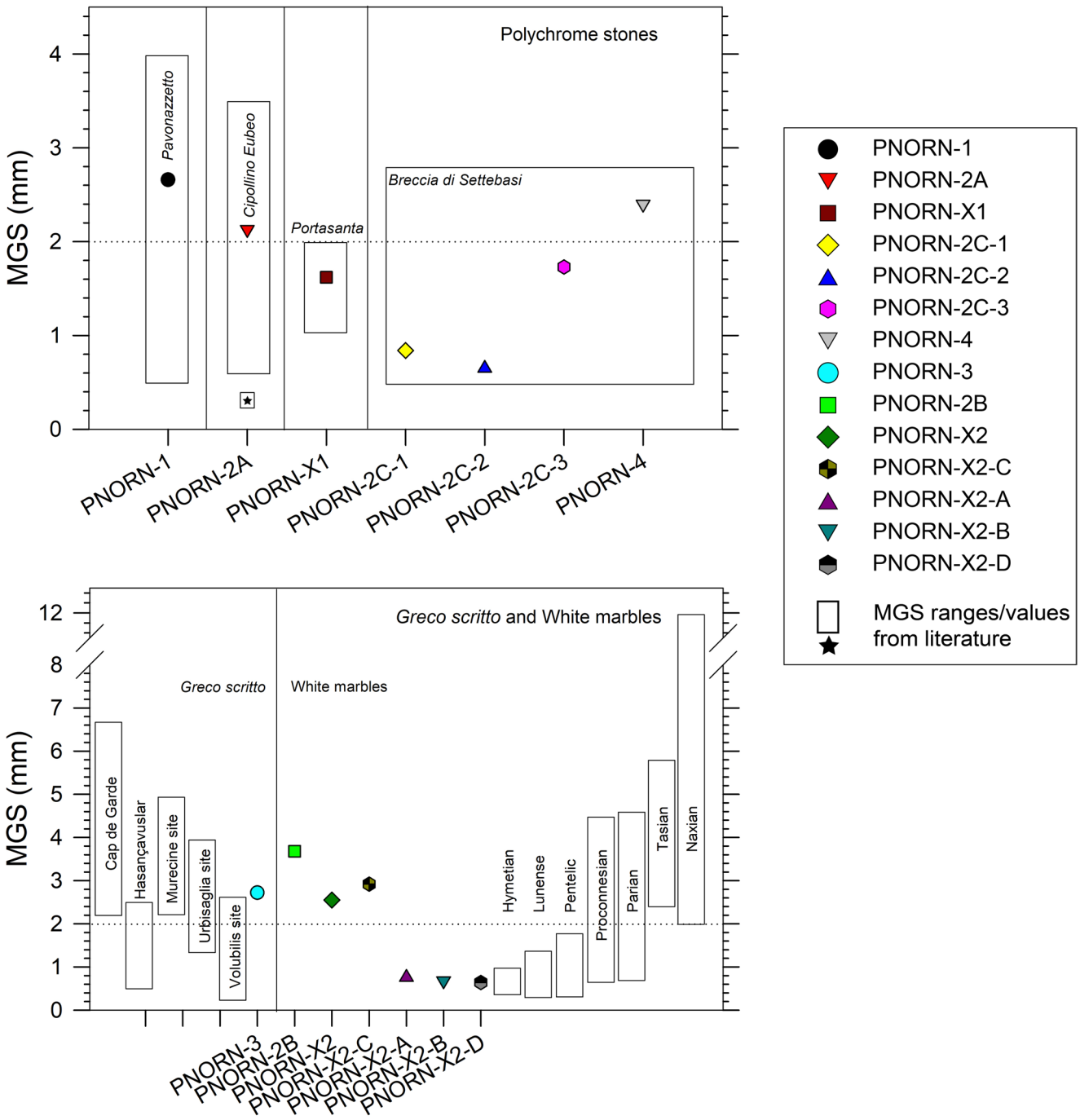

Fig. 7 Comparison of MGS values (mm) of the lithotypes investigated here (various symbols, refer to the legend) with those present in the literature, shown as boxes representing the maximum and minimum values for MGS. For *Pavonazzetto*, it refers to Çelik and Sert (2020) and Al-Bashaireh (2022). For *Cipollino verde* from Euboea, Lazzarini (2007, 2019); the black star represents the MGS value of 0.3 mm for *Cipollino* from Apuan Alps (Arnoldi et al. 1999) and those in the study of Badouna et al. (2020). For *Portasanta*, it refers to Lazzarini (2007), while for *Breccia di Settebasi* to the works of Lazzarini (2007) and Karambinis and Lazzarini (2012). *Greco Scritto* from Cap de Garde MGS values refer to Antonelli et al. (2009a), while those of Ephesian provenance (Hasançavuşlar) are from Yavuz et al. (2011). The MGS of *Greco scritto* identified at the Murecine, Urbisaglia, and Volubilis sites are from Perna et al. (2023); Antonelli and Lazzarini (2013); Antonelli et al. (2009b), respectively. For 7 of the chief white marbles used in antiquity, the database from Antonelli and Lazzarini (2015) was used

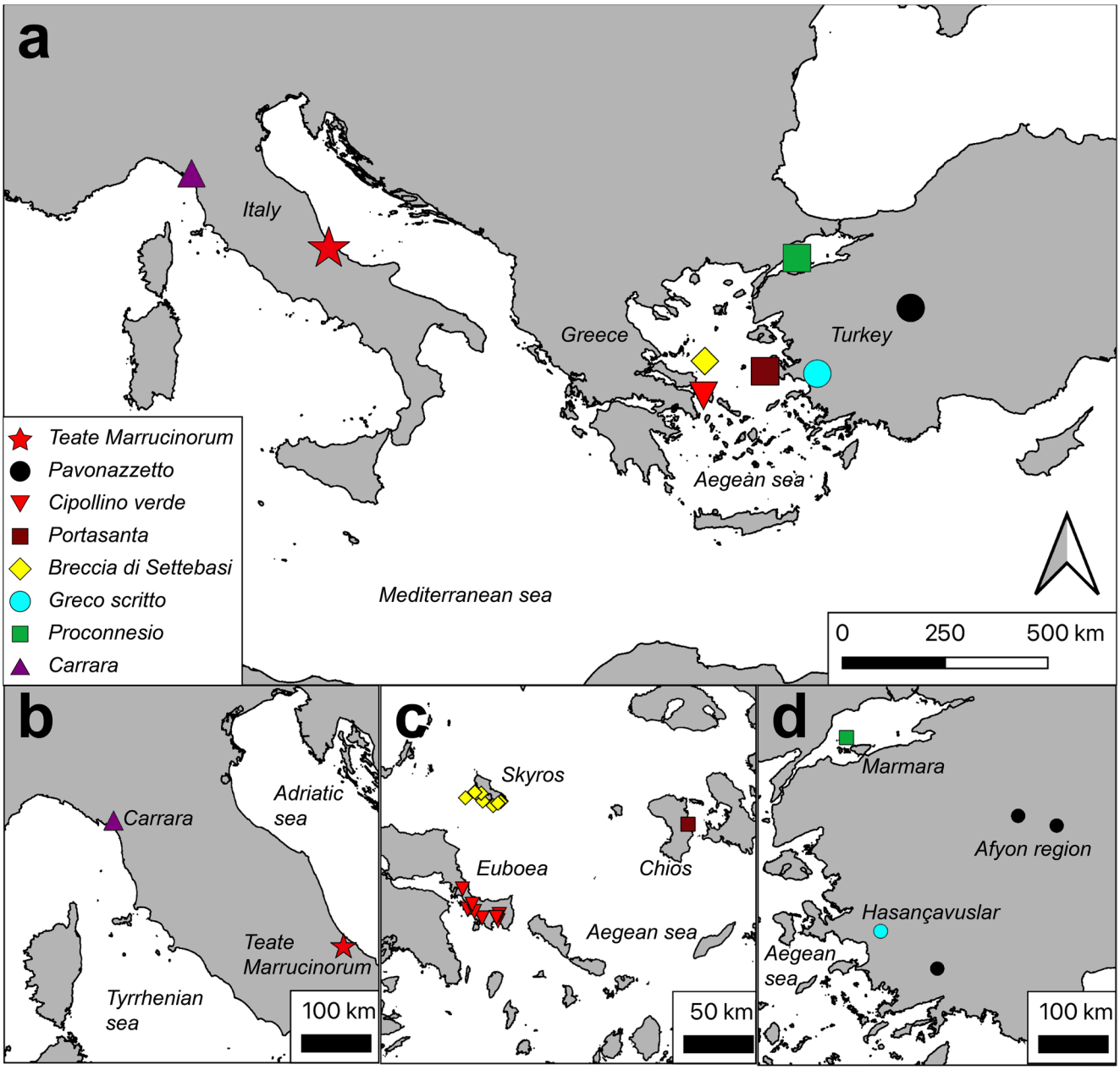

Fig. 8 (**a**) Provenance of the polychrome, grey-striped and white marble stones used as ornament of the thermal baths of *Teate Marrucinorum* (Chieti, Italy). Probable location of the quarries according to Russell (2013) for (b) Italy, (**c**) Greece and (**d**) Turkey. In Tab. S5 are reported the details of all the excavation sites

di Settebasi is more variable than the oxide ranges measured in this study (Fig. 6), proposing that an enlarged bulk geochemical characterisation of these ornamental stones could be valuable.

A similar comparison of the MGS values is presented in Fig. 7, mainly for white marbles since only a few works exist on polychrome samples (Arnoldi et al. 1999; Badouna et al. 2016, 2020; Bağci 2020; Carroll et al. 2008; Çelik and Sert 2020; Columbu et al. 2014; Lazzarini 2007). Since the MGS alone cannot discriminate a specific polychromatic lithotype, the maximum grain size values of our polychrome specimens were compared against literature data for their respective stone types. The MGS of our *Pavonazzetto* is just slightly larger than the average MGS of the white variety of the Docimium (*Pavonazzetto*) fine-grained marble, usually below 2 mm (Antonelli and Lazzarini 2015; Bağci 2020; Capedri and Venturelli 2004; Çelik and Sert 2020; Columbu et al. 2014). In addition, the MGS value of the PNORN-1 sample (Fig. 7) is well within the range of the *Pavonazzetto* stones (Al-Bashaireh 2022). Hence, the PNORN-1 sample

corresponds to the *Marmor phrigium* extracted in the Afyon region in Turkey (Al-Bashaireh 2021; Attanasio et al. 2015) (Fig. 8, Tab. S5). The MGS of other *Cipollino* stone(s), even of modern time excavations, such as those from Badouna et al. (2016, 2020) or Apuan Cipollino from Arnoldi et al. (1999), are invariably smaller than that of PNORN-2 A, being around 0.3 mm; conversely, the MGS of PNORN-2 A is indeed in the range of impure marble corresponding to the *Cipollino verde* anciently labelled *Marmor carystium* from the Euboea region in Greece (Al-Bashaireh 2022; Lazzarini 2007, 2019) (Fig. 8, Tab. S5). The maximum grain-size in sedimentary or slightly metamorphosed portions of the matrix (see above) of our PNORN-X1 *Portasanta* perfectly overlaps the measurements from literature by Lazzarini (2007) (Fig. 8). In addition, the presence of micritic clasts in which there are some ooids (Fig. S3) and the presence of quartz and dolomite (Figs. 3b, S3, S4) in both PNORN-X1 and the *Portasanta* of Lazzarini (2007) and Carroll et al. (2008) further support this conclusion, i.e. our *Portasanta* correspond to the tectonic breccia called *Marmor chium* of Romans, quarried in the Greek island of Chios (Gnoli 1988; Lazzarini 2007) (Fig. 8, Tab. S5). The equivalent of our PNORN-2 C-1, PNORN-2 C-2, PNORN-2 C-3 and PNORN-4 *Breccia di Settebasi* samples have been primarily characterised by autoptic attributes (Taelman and Antonelli 2022); to an unexperienced and untrained eye, they may show some analogies with the Italian *Breccia Medicea*, a meta-breccia quarried at Serravezza and Stazzema villages, in the Apuan Alps (Lazzarini 2019; Taelmann et al. 2019). However, an important aspect of the *Breccia Medicea* is the presence of chloritoid, that is undetected here in our PNORN-2 C-1, PNORN-2 C-2, PNORN-2 C-3 and PNORN-4 (Fig. 3, S3a, S8, S9, S10 and S11). Moreover, the MGS of our PNORN-2 C-1, PNORN-2 C-2, PNORN-2 C-3 and PNORN-4 and those of the *Breccia di Settebasi* from literature have the same minimum and maximum values (Lazzarini 2007; Karambinis and Lazzarini 2015; Fig. 7). It can be thus concluded that the four PNORN-2 C-1, PNORN-2 C-2, PNORN-2 C-3 and PNORN-4 stones from Chieti are the same meta-breccia corresponding to the ancient *Marmor scyreticum*, also known as *Breccia di Settebasi*, from the Skyros Island of Sporades in Greece (Fig. 8, Tab. S5).

As previously discussed, the MGS values of the white marbles from *Teate Marrucinorum* have been compared with those present in the literature. In particular, Fig. 7 shows 7 of the chief white marbles used in antiquity sourced from the database in Antonelli and Lazzarini (2015). The coupling of petrographic/textural and isotopic signatures, as formerly treated, pointed out that the fine-grained decorative marbles is *Marmor lunense* from Carrara in Italy (PNORN-X2-A, PNORN-X2-B, PNORN-X2-D) and medium-grained specimens are *Marmor proconnesium*, excavated in Marmara Island, Turkey (PNORN-2B, PNORN-X2, PNORN-X2-C) (Fig. 8, Tab. S5). Finally, the analysed grey-striped *Greco scritto* from Chieti (PNORN-3, PNORN-3-A, PNORN-3-B, PNORN-3-C and PNORN-3-D) show chemical compositions that are close both to that of Ephesus (Turkey) or Cap de Garde (Annaba, Algeria provenance) (Columbu et al. 2014; Gallala et al. 2017) and MGS values comparable between these two stones (Fig. 7) (Antonelli et al. 2009a, b; Yavuz et al. 2011; Antonelli and Lazzarini 2013; Columbu et al. 2014; Taelman et al. 2019; Perna et al. 2023); as previously asserted, the most suitable provenance for these marbles *s.s.* is from Hasançavuşlar (near Ephesus) in Turkey (Fig. 8, Tab. S5).

Conclusions

The ornamental stones decorating the thermal baths of *Teate Marrucinorum* are divided into three polychrome, grey-striped and white marble categories (Fig. 2). The polychrome ones are then sub-grouped into four different stones corresponding to *Pavonazzetto*, *Cipollino verde*, *Portasanta* and *Breccia di Settebasi*, according to their autoptic discrimination, while the grey-striped type corresponds to the *Greco scritto* samples (Tab. S2). Instead, the white marbles require further geochemical (Figs. 3a and 4 and Tab. S3) and petrographic (Fig. S2, Tab. S2) determinations. The two white marbles have isotopic ($\delta^{18}O$, $\delta^{13}C$) signatures (Fig. 4), MGS (Tab. S2) and microscopic features indicative of provenance from the ancient quarries of Ancient Prokonnesos in Turkey and Alpi Apuane in Italy (Tab. S5). In addition to these standard determinations, mineralogical and geochemical analyses from this study and in previous ones provide further quantitative discriminations (Tab. S3, S4 and Figs. 5, 6 and 7). This proposed new analytical approach could be extended to other ornamental stones used by the Romans to further support, corroborate, discriminate and complement autoptic conclusions on the provenance from different sites in the Mediterranean (Fig. 8).

The existing data on the thermal bath of *Teate Marrucinorum* indicate that the *Pavonazzetto* and *Greco scritto* were used to decorate two different parts of the *apodyterium*, while the same ambient of the cold tub of the *frigidarium* were covered with *Cipollino verde*, *Proconnesian* marble and *Breccia di Settebasi*, (PNORN-2 A, PNORN-2B, PNORN-2 C-1, 2 C-2 and 2 C-3); the different facies of the *Breccia di Settebasi* (PNORN-4) was used in the *tepidarium* (Fig. 1). These values of the identified Roman rocks and their provenance establishes the importance of *Teate Marrucinorum* during Imperial age.

Supplementary Information The online version contains supplementary material available at https://doi.org/10.1007/s12520-026-02487-5.

Acknowledgements Most of this study was conducted during the Ph.D. of A. Casarin; it was funded by the "Fondi Ateneo of the University G. D'Annunzio" and PRIN (2017J277S9_003) project "Time Scales of Solidification in Magmas: Application to Volcanic Eruptions, Silicate Melts, Glasses, Glass-Ceramics" awarded to G. Iezzi and to the project "DPC-ReLUIS" awarded to G. Brando. The authors are grateful to Prof. Gliozzo E. for the editorial handling and her own revision; the reviewers, Prof. Barale L., Gambino F., and an anonymous reviewer, are warmly acknowledged for the numerous fruitful comments and suggestions that improved the clarity and meaning of this study.

Author Contributions Conceptualisation: A. Casarin, G.I., F.A.; sampling: G.I., M.I.P., E.C., R.T., I.C., M.G.M., D.P., D.R.; methodology: A. Casarin, F.A., A. Cavallo, F.R., M.R.C.; data curation: A. Casarin, G.I., F.A., A. Cavallo, F.R., M.R.C., D.d.L.; writing-original draft preparation: A. Casarin, G.I., F.A.; writing-review and editing: A. Casarin, G.I., F.A., M.R.C., D.d.L., I.C., M.G.M., G.B., F.R., A. Cavallo, M.I.P., E.C., R.T., D.P., D.R.; resources: G.I., G.B., F.A., A. Cavallo, D.d.L. All authors have read and agreed to this version of the manuscript.

Funding Open access funding provided by Università degli Studi G. D'Annunzio Chieti Pescara within the CRUI-CARE Agreement.

Data Availability The authors declare that the data supporting the findings of this study are available within the paper and its supplementary information files.

Declarations

Competing interests The authors declare no competing interests.

References

Adinolfi G, Agostini S, Carmagnola R, di Carlo M, Mancini MC, Menozzi O, Palumbo D, Petraccia V (2019) Le Terme Romane di Chieti: un caso esemplificativo. https://eurotech.udanet.it/wp-content/uploads/2020/07/POSTER_TermeRomaneChieti-scaled.jpg Accessed June 2024

Agostini S (2018) The stratified growth of Chieti from roman times to tomorrow: a new, geology-based conscience in city planning and renewal. Alp Mediterr Quat 31(2):195–205. https://doi.org/10.26382/AMQ.2018.13

Agostini S, Rossi MA (2012) La presenza di marmi e pietre policrome in siti archeologici dell'Abruzzo. Quaderni Di Archeologia d'Abruzzo: Notiziario Della Soprintendenza per i Beni Archeologici Dell'Abruzzo 4:87–93. https://doi.org/10.1400/250309

Agostini S, Mariottini M, Romano J, Rossi MA (2002) Polychrome stones from the Roman baths in Chieti (Abruzzo, Italy). In: Lazzarini L (ed) Interdisciplinary studies on ancient stone: ASMOSIA VI, Proceedings of the Sixth International Conference of ASMOSIA, Association for the Study of Marble and Other Stones in Antiquity, Venice, 15–18 June 2000, pp 73–78

Akbulut ZF (2022) Experimental investigation of the surface properties of accidental stained carbonate natural stones. Case Stud Constr Mater 17:e01626. https://doi.org/10.1016/J.CSCM.2022.E01626

Al-Bashaireh K (2021) Ancient white marble trade and its provenance determination. J Archaeol Sci Rep 35:102777. https://doi.org/10.1016/J.JASREP.2020.102777

Al-Bashaireh K (2022) The white marbles and polychrome stones of the five-aisled basilica at Gadara (Umm Qais), Jordan: archaeometric characterization for provenance identification. Archaeol Anthropol Sci 14(2):1–18. https://doi.org/10.1007/s12520-021-01470-6

Antonelli F, Lazzarini L (2013) White and coloured marbles of the roman town of Urbs Salvia (Urbisaglia, Macerata, Marche, Italy). Oxf J Archaeol 32(3):293–317. https://doi.org/10.1111/ojoa.12016

Antonelli F, Lazzarini L (2015) An updated petrographic and isotopic reference database for white marbles used in antiquity. Rend Lincei 26(4):399–413. https://doi.org/10.1007/S12210-015-0423-4/

Antonelli F, Lazzarini L, Cancelliere S, Dessandier D (2009a) Minero-Petrographic and Geochemical Characterization of 'Greco Scritto' marble from Cap De Garde, near Hippo Regius (Annaba, Algeria). Archaeometry 51(3):351–365. https://doi.org/10.1111/J.1475-4754.2008.00408.X

Antonelli F, Lazzarini L, Cancelliere S, Dessandier D (2009b) Volubilis (Meknes, Morocco): Archaeometric study of the white and coloured marbles imported in the Roman age. J Cult Herit 10(1):116–123. https://doi.org/10.1016/J.CULHER.2008.04.006

Arnoldi C, Azzaro E, Barbieri M, Tucci P (1999) Petrographic and geochemical features of the Cipollino Verde marble from the Apuan Alps (northern Tuscany, Italy) and archaeometric implications. Period Miner 68:145–162

Attanasio D, Bruno M, Prochaska W, Yavuz AB (2015) Analysis and discrimination of phrygian and other pavonazzetto-like marbles. In: Pensabene P, Gasparini E (ed) Interdisciplinary studies on ancient stone: ASMOSIA X, Proceedings of the Tenth International Conference of ASMOSIA, Association for the Study of Marble & Other Stones in Antiquity, Rome, 21–26 May 2012, pp 753–764

Badouna I, Koutsovitis P, Laskaridis K, Patronis M, Papatrechas C (2016) Aesthetic characteristics of Greek ornamental stones associated with mineral, geochemical and structural properties. Bull Geol Soc Greece 50(4):1771–1780. https://doi.org/10.12681/bgsg.14104

Badouna I, Koutsovitis P, Karkalis C, Laskaridis K, Koukouzas N, Tyrologou P, Patronis M, Papatrechas C, Petrounias P (2020) Petrological and geochemical properties of Greek carbonate stones, associated with their physico-mechanical and aesthetic characteristics. Minerals 10(6):507. https://doi.org/10.3390/MIN10060507

Bağci M (2020) Mineralogical, petrographic, and geochemical characterization of colored İscehisarmarbles (Afyonkarahisar, W-Turkey). Turk J Earth Sci 29(6):946–975. https://doi.org/10.3906/yer-2001-20

Beltrame C, Percic T, Lazzarini L (2019) The archaeometric identification of the marbles of the Roman shipwrecks of Capo Granitola

(TP), Isola delle Correnti and Marzamemi I (SR). J Archaeol Sci Rep 23:953–967. https://doi.org/10.1016/J.JASREP.2018.11.021
Borghini G (ed) (1989) Marmi antichi. De Luca Edizioni D'Arte, Rome, Italy
Capedri S, Venturelli G (2004) Accessory minerals as tracers in the provenancing of archaeological marbles, used in combination with isotopic and petrographic data. Archaeometry 46(4):517–536. https://doi.org/10.1111/j.1475-4754.2004.00171.x
Carroll M, Montana G, Randazzo L, Giarrusso R (2008) Recovering evidence for the use of marble and coloured limestone in the first century AD in excavations at the sanctuary of Venus in Pompeii. Fasti Line Documents Res 119:281–311
Çelik MY, Sert M (2020) The importance of "Pavonazzetto marble" (Docimium-Phrygia/Iscehisar-Turkey) since ancient times and its properties as a global heritage stone resource. Environ Earth Sci 79(9):1–18. https://doi.org/10.1007/S12665-020-08943-2/
Chipera SJ, Bish DL (2013) Fitting Full X-Ray Diffraction Patterns for Quantitative Analysis: A Method for Readily Quantifying Crystalline and Disordered Phases. Adv Mater Phys Chem 03(01):47–53. https://doi.org/10.4236/ampc.2013.31a007
Columbu S, Antonelli F, Lezzerini M, Miriello D, Adembri B, Blanco A (2014) Provenance of marbles used in the Heliocaminus Baths of Hadrian's Villa (Tivoli, Italy). J Archaeol Sci 49(1):332–342. https://doi.org/10.1016/J.JAS.2014.05.026
Corsi F (1845) Delle Pietre Antiche. Dalla Tipografia Salviucci, Rome, Italy
Della Ventura G, Iezzi G, Redhammer GJ, Hawthorne FC, Scaillet B, Novembre D (2005) Synthesis and crystal-chemistry of amphiboles along the magnesioriebeckite – magnesio-arfvedsonite series as a function of fO_2. Am Mineral 90:1375–1383. https://doi.org/10.2138/am.2005.1682
European Commission - Extra-Expo project (2015) Marble, the divine stone. Its extraction, trade and use since the beginning of the humanity until the present
Fettes D, Desmons J (2007) Metamorphic Rocks: a classification and glossary of terms. Cambridge University Press
Galderisi A, Iezzi G, Bianchini G, Paris E, de Brito J (2022) Petrography of construction and demolition waste (CDW) from Abruzzo region (Central Italy). Waste Manag 137:61–71. https://doi.org/10.1016/J.WASMAN.2021.10.028
Gallala W, Younès A, Gaied ME, Hadjzobir S, Sparks K, Molli G (2017) A multi-analytical approach for determining the provenance of the marbles from Ruspina Roman baths (Monastir, Tunisia). Archaeol Anthropol Sci 9(6):1275–1285. https://doi.org/10.1007/S12520-016-0323-2/
Gnoli R (1988) Marmora romana. Edizioni dell'Elefante, Rome, Italy
Hubbard CR, Snyder RL (1988) RIR - measurement and use in quantitative XRD. Powder Diffr 3(2):74–77. https://doi.org/10.1017/S0885715600013257
Iezzi G, Della Ventura G, Cámara F, Pedrazzi G, Robert JL (2003) ^{B}Na–^{B}Li solid-solution in A-site-vacant amphiboles: synthesis and cation ordering along the ferri-clinoferroholmquistite–riebeckite join. Am Mineral 88(7):955–961. https://doi.org/10.2138/am-2003-0702
ISPRA (2012) Carta Geologica d'Italia alla scala 1:50.000, Progetto CARG. Foglio n. 361 Chieti. Servizio Geologico d'Italia
Karambinis M, Lazzarini L (2015) The Roman marble quarries of Aliko Bay and of the islets of Rinia and Koulouri (Skyros, Greece). In: Pensabene P, Gasparini E (ed) Interdisciplinary studies on ancient stone: ASMOSIA X, Proceedings of the Tenth International Conference of ASMOSIA, Association for the Study of Marble & Other Stones in Antiquity, Rome, 21–26 May 2012, pp 791–804
Lazzarini L (2007) Poikiloi Lithoi, Versiculores Maculae: i marmi colorati della Grecia Antica: storia, uso, diffusione, cave, geologia, caratterizzazione scientifica, archeometria, deterioramento. Serra F (Ed)
Lazzarini L (2019) Ancient Mediterranean polychrome stones. In: Artioli G, Oberti R (ed) The Contribution of Mineralogy to Cultural Heritage. EMU Notes in Mineralogy, Vol. 20, pp. 367–392. Mineralogical Society of Great Britain and Ireland. https://doi.org/10.1180/EMU-notes.20.10
McCrea JM (1950) On the isotopic chemistry of carbonates and a paleotemperature scale. J Chem Phys 18(6):849–857. https://doi.org/10.1063/1.1747785
Pensabene P (1993) Marmi antichi. Problemi d'impiego, di restauro e d'identificazione. L'Erma di Bretschneider, Rome, Italy
Pensabene P (2002) Committenza edilizia a Ostia tra la fine del I e i primi decenni del III secolo. Lo studio dei marmi e della decorazione architettonica come strumento d'indagine. Mélanges de l'École Française de Rome Antiquité 114(1):181–324. https://doi.org/10.3406/mefr.2002.10698
Perna S, Antonelli F, Lazzarini L (2023) Archaeometric analysis of the 'greco scritto' marble slabs from the Edificio dei Triclinii at Murecine (Pompeii, Italy). Archaeometry 65(1):1–16. https://doi.org/10.1111/arcm.12811
Potere D, Iezzi G, Scisciani V, Tangari AC, Nazzari M (2023) Provenance and deposition of a lithified volcanic-rich layer (VRL-5.5) at 5.5 Ma from Central Apennines (Italy). Sci Rep 13:6880. https://doi.org/10.1038/s41598-023-33256-2
Radica F, Casarin A, Iezzi G, Bravo M, de Brito J, Galderisi A, Brando G, Nazzari M, Scarlato P (2024) Cement vs aggregates and textures of aggregates in a mortar: comparative image analysis methods and analytical protocols. Constr Build Mater 453:139033. https://doi.org/10.1016/J.CONBUILDMAT.2024.139033
Russell B (2013) Gazetteer of Stone Quarries in the Roman World. Version 1.0. Data set/Database: http://oxrep.classics.ox.ac.uk/databases/stone_quarries_database/
Taelman D, Antonelli F (2022) Provenance of the white and polychrome marbles used for the architecture and sculpture of roman Sentinum (Sassoferrato, Marche, Italy). Archaeometry 64(1):1–24. https://doi.org/10.1111/arcm.12690
Taelman D, Delpino C, Antonelli F (2019) Marble decoration of the Roman theatre of Urvinum Mataurense (Urbino, Marche region, Italy): An archaeological and archaeometric multi-method provenance study. J Cult Herit 39:238–250. https://doi.org/10.1016/j.culher.2019.03.009
Taelman D, Mei O, Antonelli F (2023) On the Use of White Marbles in Roman Forum Sempronii (Fossombrone, Marche, Italy): An Overview of the Archaeometric Data on Architectural Elements. Heritage 6(3):2942–2955. https://doi.org/10.3390/HERITAGE6030156
Tarquini S, Isola I, Favalli M, Battistini A, Dotta G (2023) TINITALY, a digital elevation model of Italy with a 10 meters cell size (Version 1.1). Istituto Nazionale di Geofisica e Vulcanologia (INGV) https://doi.org/10.13127/tinitaly/1.1
Yavuz AB, Bruno M, Attanasio D (2011) An updated, multi-method database of Ephesos marbles, including White, Greco Scritto and Bigio varieties. Archaeometry 53(2):215–240. https://doi.org/10.1111/j.1475-4754.2010.00542.x